A noise-driven oscillator explains the universal 1/f-like behavior of neural field spectra

Mark A. Kramer
Department of Mathematics and Statistics, and Center for Systems Neuroscience
Boston University, Boston MA, 02214

Catherine J. Chu
Department of Neurology
Massachusetts General Hospital and Harvard Medical School, Boston MA, 02114

ABSTRACT

Consistent observations across recording modalities, experiments, and neural systems find neural field spectra with 1/f-like scaling, eliciting many alternative theories to explain this universal phenomenon. We propose a simple generative mechanism with equivalent physical and statistical interpretations. This framework demonstrates how correlated and uncorrelated noise generate 1/f-like spectra consistent with *in vivo* observations, without requiring a specific biological mechanism or collective critical behavior.

INTRODUCTION

Transient oscillations are a prominent feature of macroscopic neural field activity [1], linked to brain function [2] and dysfunction [3], [4]. Oscillations appear as narrowband increases in the spectrum above an aperiodic background in which the power P decreases proportional to the frequency f raised to an exponent β: $P \propto f^{\beta}$. Sophisticated methods [5]–[7] support estimation of the 1/f-like, scale-free [8] or power-law [9] behavior of neural field spectra. Changes in β, the aperiodic exponent, have been investigated in many domains, including sleep [10]–[13], aging [14]–[16], and disease [17]–[19]. While many factors impact estimation of the aperiodic exponent (e.g., the frequency range analyzed [20], [21]), values of the exponent reported at higher frequencies (>20 Hz) typically range between -4 and -2 (Table 1).

The universal observation of 1/f-like neural field spectra with a restricted range of aperiodic exponents across different recording modalities, experiments, and neural systems suggests a simple generative mechanism. However, many complex, specific mechanisms have been identified to generate this phenomenon. These include excitatory/inhibitory balance [22], low-pass frequency filtering by dendrites [23] or the extracellular medium [24], nonideal resistive components in the cell membrane [25], stochastic firing of neurons convolved with an exponential relaxation process [24], [26], [27], stochastic synaptic conductances [28], stochastically driven damped oscillators with different relaxation rates [29], local homogenous connectivity [30], combinations of many transient oscillations at different frequencies and amplitudes [31], or network mechanisms linking slower rhythms to broad neuronal recruitment and therefore larger amplitude field potentials [23]. Theoretically, scale-free phenomena – with 1/f-like behavior – have been linked to fractal properties [32], critical transitions [9], [33], and self-organized criticality [34], [35]. How these proposed biological and mathematical mechanisms contribute – separately or combined – to the range of aperiodic exponents observed across diverse neural field spectra remains unclear.

Here, we propose a simple generative mechanism for the 1/f-like behavior observed at higher frequencies (>20 Hz) in neural field spectra. Two noise terms – representing correlated and uncorrelated noise inputs – determine the value of the aperiodic exponent β. Two equivalent interpretations of the model exist, as either a mechanistic or statistical process. We propose that this simple model implements general physical and statistical properties to capture a broad range of aperiodic exponents observed *in vivo*, without requiring a specific biological mechanism or tuning to collective critical behavior.

RESULTS

As a generative model of the neural population voltage (V) we consider:

$$C\frac{dV}{dt} = I + \epsilon_V$$
$$\frac{dI}{dt} = -\delta I - \omega_0^2 V + \epsilon_I \ .$$

In the first equation, an input current (I) and voltage noise (ϵ_V, Gaussian distributed with mean 0 and variance σ_V^2) drive changes in the voltage V. In the second equation damping (δ) and a natural oscillatory mechanism ($\omega_0 = 2\pi f_0$) resist changes in the current, while current noise (ϵ_I, Gaussian distributed with mean 0 and variance σ_I^2) drives changes in the current.

This generative model produces aperiodic exponents (β) between -4 and -2. We illustrate the dynamics as the voltage noise ϵ_V increases from 0 by performing numerical simulations of the generative model and estimating the aperiodic exponent β (at frequencies between 20 Hz and 250 Hz). As ϵ_V increases, the aperiodic exponent increases from $\beta = -4$ until $\beta = -2$ (Figure 1), consistent with the diversity of values reported in the literature (Table 1).

Analysis of the generative model in the limiting cases of $\beta \approx -4$ and $\beta \approx -2$ provides insights into the physical and statistical mechanisms producing the aperiodic exponents observed (see Methods). When $\beta \approx -4$, the model reduces to a damped oscillator driven by noise, which is equivalent to an autoregressive model of order 2 (or AR(2), see for example [36]). When $\beta \approx -2$, a random walk dominates the voltage dynamics at high frequencies, which is equivalent to an autoregressive model of order 1 (or AR(1), see for example [37]). These autoregressive models provide alternative generative mechanisms for understanding the limiting values of the aperiodic exponents reported in the literature: the voltage now (at discrete time index t) is a function of its recent history (at times $t-1$ when $\beta \approx -2$, and at times $t-1, t-2$ when $\beta \approx -4$) plus noise.

To summarize, the 1/f-like scaling of neural field spectra can be explained by a simple generative mechanism driven by two types of Gaussian noise. For this model, the spectrum consists of a single, broad peak at the natural frequency of the neural population (f_0). At high frequencies, when $f \gg f_0$, the aperiodic exponent varies between $\beta = -4$ and $\beta = -2$ depending on the voltage noise.

DISCUSSION

A universal feature of neural field potential spectra is 1/f-like scaling. To produce this power-law, many generative mechanisms have been proposed with diverse biological implementations and interpretations. Here, we instead propose a general generative mechanism and model neural population activity driven by two types of noise. This simplicity results in a more parsimonious model (i.e., a model with few parameters) that produces rhythmic time series with aperiodic exponents between -4 and -2, consistent with the range of values reported *in vivo* for higher frequencies (e.g., >20 Hz) across recording modalities, experiments, and neural systems.

Under the proposed generative mechanism, the range of aperiodic exponents reflects different types of neural noise. We note that the voltage dynamics depend directly on the voltage noise ϵ_V and indirectly on the current noise ϵ_I. The current dynamics introduce correlations in the uncorrelated current noise before this noise reaches the voltage dynamics. Therefore, the voltage dynamics depend on both uncorrelated and correlated noise inputs, and we may interpret the aperiodic exponent in terms of these different types of noise; an aperiodic exponent near $\beta = -4$ indicates correlated noise inputs dominate the high frequency voltage dynamics, while $\beta = -2$ indicates uncorrelated noise dominates the high frequency voltage dynamics.

The generative model proposed here shares similarities with existing model proposals. The model is similar in form to single-compartment neuron models developed to characterize membrane potential fluctuations [28]. In those models, voltage changes depend on synaptic conductances with noise-driven dynamics. Here, voltage changes depend on two types of noise, passed through an oscillatory linear dynamical system, to produce the range of aperiodic exponents observed. A similar range of aperiodic exponents (between -4 and -2) was identified in a computational model of membrane potential fluctuations [25]. In this model, the authors extend the cable equation to include a nonideal resistance component, representing the resistance of the membrane to lateral ion displacements. Increasing values of the relaxation time associated with this additional resistance increased the

aperiodic exponent. If this membrane property changes with brain state (e.g., wakefulness versus sleep) then it may also contribute to the range of aperiodic exponents observed at the neural population scale. Finally, we note that the aperiodic exponent of $\beta = -4$ with no voltage noise is expected and persists for more complicated nonlinear systems [38]. Unlike this previous work, we consider here two types of stochastic forcing (ϵ_V and ϵ_I) which we show numerically supports estimated aperiodic exponents across the entire continues range of -4 to -2.

Some observations report aperiodic exponents greater than -2 (i.e., $\beta > -2$). Experimental factors, such as measurement noise which flattens the spectrum and shifts β towards 0, might contribute to these observations. In addition, analysis factors may impact reported results. For example, the frequency range considered varies widely across studies (see discussion of fitting ranges in [21]). In general, larger aperiodic exponents (more negative β) occur at higher frequencies [24], [39]–[41], although not always [42]. For the generative model proposed here, the result $-4 \leq \beta \leq -2$ holds in the high frequency limit, when the measured frequency exceeds the natural frequency of the neural population. Analyzing lower frequency bands (e.g., below the broadband peak), or analyzing the low and high frequency bands after accounting for the broadband peak, increases the exponent in this model. In the model, when the observed frequency is much less than the natural frequency ($f \ll f_0$) the power approaches a constant with aperiodic exponent $\beta = 0$. While potentially useful, the aperiodic exponent reported in lower frequency bands is more difficult to interpret. To assess low frequency rhythms requires long durations of data, which increases the chance of non-stationarities. Artifacts (e.g., slow drifts) and analysis choices (e.g., whether to subtract the signal mean) also impact the low frequency power. Finally, while power-law features at low frequencies may reflect the same power-law features at high frequencies, these different phenomena unlikely reflect the same neural mechanisms.

Many well-supported observations of power-laws appear in neuroscience (e.g., avalanches of population voltage discharges [43], amplitudes of narrowband oscillations [44]). Here, we consider one type of power-law: the 1/f-like neural field spectrum and propose a simple, noise-driven generative mechanism. Under this model, the aperiodic exponent represents two types of neural noise, without requiring a sophisticated biological or dynamical mechanism. Equivalently, the aperiodic exponent reflects a characteristic timescale of the signal; the aperiodic exponent decreases (β becomes more negative) with increasing history dependence. This simple interpretation requires no specific mechanism; the aperiodic exponent simply captures the history dependence of the signal. The model simplicity is consistent with the universality of 1/f-like field spectra, reflecting a basic feature of spontaneous neural noise beyond neural oscillations. However, this simplicity may also limit the computational utility of this mechanism and the role of the aperiodic exponent in measuring neural computations. We conclude that the most parsimonious explanation of 1/f-like neural field spectra is just (two types) of noise.

Table 1: Example aperiodic exponents for human voltage spectra reported in the literature*. The mean value of the aperiodic exponent (β) reported in the reference listed in column Ref. Additional details include the year of study, recording modality, number of subjects n and additional subject information, frequency range analyzed, and experimental condition. Considering only those studies with minimum frequencies >20 Hz (yellow highlighted rows), the aperiodic exponent has mean -3.1, lower quartile -4, and upper quartile -2.5.*

β	Ref	Year	Recording modality	Frequency	Experimental condition
-0.08	[39]	2019	Scalp EEG (n=5)	20-40 Hz	Anesthesia (Ketamine)
-1.12	[19]	2022	Scalp EEG (n=16, control subjects)	1-40 Hz	Eyes closed
-1.3	[45]	2021	Scalp EEG (n=74, Tourette syndrome)	2-40 Hz	Behavioral experiments
-1.44	[45]	2021	Scalp EEG (n=74, control)	2-40 Hz	Behavioral experiments
-1.48	[19]	2022	Scalp EEG (n=18, stroke patients)	1-40 Hz	Stroke patients
-1.51	[18]	2019	Scalp EEG (n=78, control subjects)	4-50 Hz	Resting state
-1.67	[18]	2019	Scalp EEG (n=76, ADHD subjects)	4-50 Hz	Resting state
-1.84	[10]	2020	Scalp EEG (n=9)	30-45 Hz	Wakefulness
-1.86	[46]	2013	Scalp EEG (n=7, adults)	0.2-30 Hz	Sleep
-1.87	[10]	2020	Scalp EEG (n=14)	30-45 Hz	Resting state
-2.03	[39]	2019	Scalp EEG (n=5)	20-40 Hz	Wakefulness
-2.07	[46]	2013	Scalp EEG (n=15, newborns)	0.2-30 Hz	Sleep
-2.32	[47]	2000	Intracranial EEG (n=5)	0.5-150 Hz	Resting state
-2.33	[12]	2021	Scalp EEG (n=175, T5)	2-48 Hz	NREM sleep
-2.44	[31]	2010	Intracranial EEG (n=5)	1-100 Hz	Wakefulness
-2.48	[39]	2019	Scalp EEG (n=5)	20-40 Hz	Wakefulness
-2.71	[11]	2022	Scalp EEG (n=251)	2-48 Hz	NREM sleep
-2.73	[12]	2021	Scalp EEG (n=175, Fz)	2-48 Hz	NREM sleep
-2.75	[10]	2020	Intracranial EEG (n=12)	30-45 Hz	Wakefulness
-2.87	[31]	2010	Intracranial EEG (n=5)	1-100 Hz	Slow wave sleep
-2.99	[10]	2020	Intracranial EEG (n=10)	30-45 Hz	Wakefulness
-3.1	[10]	2020	Scalp EEG (n=9)	30-45 Hz	Anesthesia
-3.13	[39]	2019	Scalp EEG (n=5)	20-40 Hz	Wakefulness
-3.46	[10]	2020	Scalp EEG (n=14)	30-45 Hz	N3 Sleep
-3.59	[39]	2019	Scalp EEG (n=5)	20-40 Hz	Anesthesia (Xenon)
-3.67	[10]	2020	Scalp EEG (n=14)	30-45 Hz	N2 Sleep
-3.69	[10]	2020	Intracranial EEG (n=10)	30-45 Hz	N3 Sleep
-4	[27]	2009	Intracranial EEG (n=20)	80-500 Hz	Behavioral experiments
-4.15	[10]	2020	Intracranial EEG (n=10)	30-45 Hz	REM sleep
-4.34	[10]	2020	Intracranial EEG (n=12)	30-45 Hz	Anesthesia
-4.36	[39]	2019	Scalp EEG (n=5)	20-40 Hz	Anesthesia (Propofol)
-4.73	[10]	2020	Scalp EEG (n=14)	30-45 Hz	REM sleep

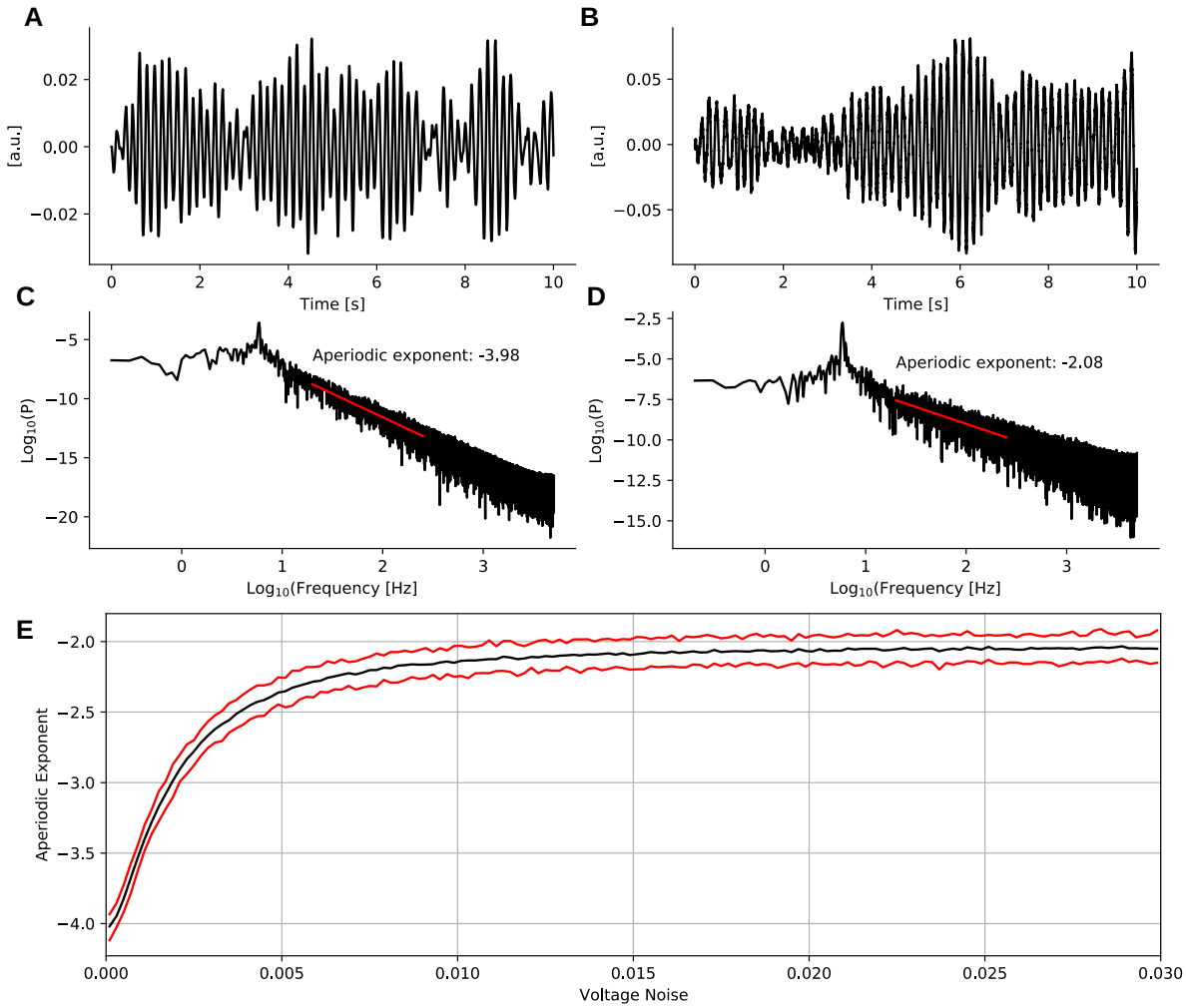

Figure 1: The aperiodic exponent increases from approximately -4 to -2 with the voltage noise. (A,B) *Example voltage time series when (A) the voltage noise is 0 (i.e., $\epsilon_V = 0$), or (B) the voltage noise is non-zero (i.e., $\sigma_V = 0.03$). A rhythm at the natural frequency ($f_0 = 6$ Hz) dominates each time series.* ***(C,D)*** *The corresponding spectra (black) and linear fits (red, 20 Hz to 250 Hz) for the time series in (A,B).* ***(E)*** *Estimates of the aperiodic exponent for increasing values of voltage noise. Black (red) indicates mean (standard deviation) of estimates across 100 simulations. In all simulations, the current noise ($\sigma_I = 1$) and damping coefficient ($\delta = 1$) are fixed. Code to simulate the model and create this figure is available at https://github.com/Mark-Kramer/Aperiodic-Exponent-Model.*

METHODS

Analysis of the generative model in the limiting case of $\beta \approx -4$

We consider a neural population with no voltage noise ($\epsilon_V = 0$), and combine the two generative model equations to find,

$$\frac{d^2V}{dt^2} = -\delta \frac{dV}{dt} - \omega_0^2 V + \epsilon_I \,. \tag{1}$$

Equation (1) describes a damped oscillator driven by noise. The current noise ϵ_I drives the voltage dynamics and, in response to this drive, the voltage oscillates (centered at frequency $\omega_0 = 2\pi f_0$) with activity damped by a resistive force (strength determined by δ). Consistent with *in vivo* observations and more complex models of large-scale neural activity [29], [48]–[52], this generative model produces damped or persistent oscillations (depending on the magnitude of the damping coefficient δ) with a broadband spectral peak centered at f_0 Hz.

To understand the spectrum of (1), we note that the spectrum of a damped oscillator driven by a sinusoidal driving force with frequency f is (see, for example, [53]),

$$P \propto \frac{1}{(f_0^2 - f^2)^2} \,. \tag{2}$$

We see from (2) that the power P is large when $f = f_0$; a resonance (i.e., a large amplitude response) occurs in the neural field when the sinusoidal driving frequency equals the natural frequency of the damped oscillator ($f = f_0$). Interpreting the noise (ϵ_I) as a wideband driving force, with non-zero power at all frequencies, we expect the spectrum of (1) to follow (2) so that,

$$P \propto \frac{1}{f^4} \,,$$

at high frequencies (i.e., frequencies much greater than the natural frequency, $f \gg f_0$). We conclude that, in the case of no voltage noise, the aperiodic exponent of the model approaches $\beta = -4$.

Analysis of the generative model in the limiting case of $\beta \approx -2$

We consider the generative model with voltage noise ($\epsilon_V \neq 0$). If there were no driving current (I fixed at 0), then the generative model becomes,

$$\frac{dV}{dt} = \epsilon_V \,,$$

so that the voltage dynamics follow a random walk. In this case, the spectrum (see, for example [37]) is,

$$P \propto \frac{1}{f^2} \,.$$

If instead we allow a driving current (I not fixed at 0), then we expect low frequency dynamics consistent with a damped oscillator driven by noise; i.e., at low frequencies, we expect a peak in the spectrum (or resonance) at the natural frequency f_0 of the neural population. However, at high frequencies ($f \gg f_0$), we expect the random walk dynamics to dominate the spectrum because $f^{-2} \gg f^{-4}$. We conclude that, in the case of non-zero voltage noise, the aperiodic exponent of the generative model approaches $\beta = -2$.

Estimation of the aperiodic exponent β from time series data

To estimate the aperiodic exponent β, we first compute the spectrum in the standard way. To a simulated voltage time series (V_t) with sampling interval $\Delta = 0.0001$ s and duration $T = 10$ s, we subtract the mean, apply a Hanning taper, compute the Fourier transform (V_f), and multiply by the complex conjugate (V_f^*):

$$P = \frac{2\,\Delta^2}{T}\, V_f\, V_f^* \,.$$

We note that the square of the Fourier coefficients is essential for consistent interpretation of the aperiodic exponent across studies; omitting the square is a common mistake identified in previous work (see discussion in [37]). For frequencies f between 20 Hz and 250 Hz, we fit a linear model to the logarithm base 10 of the spectrum ($\log_{10} P$) with predictor logarithm base 10 of the frequency ($\log_{10} f$),

$$\log_{10} P = c + \beta \log_{10} f \,,$$

where β is the estimate of the aperiodic exponent. Code to compute the spectrum is available at https://github.com/Mark-Kramer/Aperiodic-Exponent-Model.

REFERENCES

[1] G. Buzsaki, *Rhythms of the Brain*. Oxford University Press, 2011.

[2] G. Buzsaki and A. Draguhn, “Neuronal Oscillations in Cortical Networks,” *Science*, vol. 304, no. 5679, pp. 1926–1929, Jun. 2004, doi: 10.1126/science.1099745.

[3] P. J. Uhlhaas and W. Singer, “Neuronal Dynamics and Neuropsychiatric Disorders: Toward a Translational Paradigm for Dysfunctional Large-Scale Networks,” *NEURON*, vol. 75, no. 6, pp. 963–980, Sep. 2012.

[4] Gibbs and Lennox, “Epilepsy: a paroxysmal cerebral dysrhythmia,” *Epilepsy & behavior : E&B*, vol. 3, no. 4, pp. 395–401, Aug. 2002.

[5] T. Donoghue *et al.*, “Parameterizing neural power spectra into periodic and aperiodic components,” *Nat Neurosci*, vol. 23, no. 12, pp. 1655–1665, Dec. 2020, doi: 10.1038/s41593-020-00744-x.

[6] H. Wen and Z. Liu, “Separating Fractal and Oscillatory Components in the Power Spectrum of Neurophysiological Signal,” *Brain Topogr*, vol. 29, no. 1, pp. 13–26, Jan. 2016, doi: 10.1007/s10548-015-0448-0.

[7] L. E. Wilson, J. da Silva Castanheira, and S. Baillet, “Time-resolved parameterization of aperiodic and periodic brain activity,” *eLife*, vol. 11, p. e77348, Sep. 2022, doi: 10.7554/eLife.77348.

[8] B. J. He, “Scale-free brain activity: past, present, and future,” *Trends in Cognitive Sciences*, vol. 18, no. 9, pp. 480–487, Sep. 2014, doi: 10.1016/j.tics.2014.04.003.

[9] M. Newman, “Power laws, Pareto distributions and Zipf’s law,” *Contemporary Physics*, vol. 46, no. 5, pp. 323–351, Sep. 2005, doi: 10.1080/00107510500052444.

[10] J. D. Lendner *et al.*, “An electrophysiological marker of arousal level in humans,” *eLife*, vol. 9, p. e55092, Jul. 2020, doi: 10.7554/eLife.55092.

[11] C. G. Horváth *et al.*, “Overnight dynamics in scale-free and oscillatory spectral parameters of NREM sleep EEG,” *Sci Rep*, vol. 12, no. 1, Art. no. 1, Nov. 2022, doi: 10.1038/s41598-022-23033-y.

[12] R. Bódizs *et al.*, “A set of composite, non-redundant EEG measures of NREM sleep based on the power law scaling of the Fourier spectrum,” *Sci Rep*, vol. 11, no. 1, p. 2041, Jan. 2021, doi: 10.1038/s41598-021-81230-7.

[13] W. J. Freeman and J. Zhai, “Simulated power spectral density (PSD) of background electrocorticogram (ECoG),” *Cogn Neurodyn*, vol. 3, no. 1, pp. 97–103, Mar. 2009, doi: 10.1007/s11571-008-9064-y.

[14] N. Schaworonkow and B. Voytek, “Longitudinal changes in aperiodic and periodic activity in electrophysiological recordings in the first seven months of life,” *Developmental Cognitive Neuroscience*, vol. 47, p. 100895, Feb. 2021, doi: 10.1016/j.dcn.2020.100895.

[15] B. Voytek *et al.*, “Age-Related Changes in 1/f Neural Electrophysiological Noise,” *J. Neurosci.*, vol. 35, no. 38, pp. 13257–13265, Sep. 2015, doi: 10.1523/JNEUROSCI.2332-14.2015.

[16] E. Cesnaite *et al.*, “Alterations in rhythmic and non-rhythmic resting-state EEG activity and their link to cognition in older age,” *NeuroImage*, vol. 268, p. 119810, Mar. 2023, doi: 10.1016/j.neuroimage.2022.119810.

[17] T. Numan *et al.*, “Regional healthy brain activity, glioma occurrence and symptomatology,” *Brain*, vol. 145, no. 10, pp. 3654–3665, Oct. 2022, doi: 10.1093/brain/awac180.

[18] M. M. Robertson, S. Furlong, B. Voytek, T. Donoghue, C. A. Boettiger, and M. A. Sheridan, “EEG power spectral slope differs by ADHD status and stimulant medication exposure in early childhood,” *Journal of Neurophysiology*, vol. 122, no. 6, pp. 2427–2437, Dec. 2019, doi: 10.1152/jn.00388.2019.

[19] J. Lanzone *et al.*, “EEG spectral exponent as a synthetic index for the longitudinal assessment of stroke recovery,” *Clinical Neurophysiology*, vol. 137, pp. 92–101, May 2022, doi: 10.1016/j.clinph.2022.02.022.

[20] M. P. H. Stumpf and M. A. Porter, “Critical Truths About Power Laws,” *Science*, vol. 335, no. 6069, pp. 665–666, Feb. 2012, doi: 10.1126/science.1216142.

[21] M. Gerster *et al.*, “Separating Neural Oscillations from Aperiodic 1/f Activity: Challenges and Recommendations,” *Neuroinform*, vol. 20, no. 4, pp. 991–1012, Oct. 2022, doi: 10.1007/s12021-022-09581-8.

[22] R. Gao, E. J. Peterson, and B. Voytek, “Inferring synaptic excitation/inhibition balance from field potentials,” *NeuroImage*, vol. 158, pp. 70–78, Sep. 2017, doi: 10.1016/j.neuroimage.2017.06.078.

[23] G. Buzsáki, C. Anastassiou, and C. Koch, “The origin of extracellular fields and currents — EEG, ECoG, LFP and spikes,” *Nature Reviews Neuroscience*, vol. 13, no. 6, pp. 407–420, Jan. 2012, doi: 10.1038/nrn3241.

[24] C. Bédard, H. Kröger, and A. Destexhe, “Does the 1/f frequency scaling of brain signals reflect self-organized critical states?,” *Physical Review Letters*, vol. 97, no. 11, p. 118102, Sep. 2006.
[25] C. Bédard and A. Destexhe, “A Modified Cable Formalism for Modeling Neuronal Membranes at High Frequencies,” *Biophysical Journal*, vol. 94, no. 4, pp. 1133–1143, Feb. 2008, doi: 10.1529/biophysj.107.113571.
[26] J. Milstein, F. Mormann, I. Fried, and C. Koch, “Neuronal shot noise and Brownian 1/f2 behavior in the local field potential,” *PLoS ONE*, vol. 4, no. 2, p. e4338, 2009.
[27] K. Miller, L. Sorensen, J. Ojemann, and M. den Nijs, “Power-Law Scaling in the Brain Surface Electric Potential,” *PLoS Comput Biol*, vol. 5, no. 12, p. e1000609 EP, Dec. 2009, doi: 10.1371/journal.pcbi.1000609.
[28] M. Rudolph, J. G. Pelletier, D. Paré, and A. Destexhe, “Characterization of Synaptic Conductances and Integrative Properties During Electrically Induced EEG-Activated States in Neocortical Neurons In Vivo,” *Journal of Neurophysiology*, vol. 94, no. 4, pp. 2805–2821, Oct. 2005, doi: 10.1152/jn.01313.2004.
[29] R. Evertz, D. G. Hicks, and D. T. J. Liley, “Alpha blocking and 1/fβ spectral scaling in resting EEG can be accounted for by a sum of damped alpha band oscillatory processes,” *PLOS Computational Biology*, vol. 18, no. 4, p. e1010012, Apr. 2022, doi: 10.1371/journal.pcbi.1010012.
[30] V. K. Jirsa, “Neural field dynamics with local and global connectivity and time delay,” *Philos Trans A Math Phys Eng Sci*, vol. 367, no. 1891, pp. 1131–1143, Mar. 2009, doi: 10.1098/rsta.2008.0260.
[31] B. J. He, J. M. Zempel, A. Z. Snyder, and M. E. Raichle, “The temporal structures and functional significance of scale-free brain activity,” *NEURON*, vol. 66, no. 3, pp. 353–369, May 2010, doi: 10.1016/j.neuron.2010.04.020.
[32] W. S. Pritchard, “The Brain in Fractal Time: 1/F-Like Power Spectrum Scaling of the Human Electroencephalogram,” *International Journal of Neuroscience*, vol. 66, no. 1–2, pp. 119–129, Jan. 1992, doi: 10.3109/00207459208999796.
[33] J. O’Byrne and K. Jerbi, “How critical is brain criticality?,” *Trends in Neurosciences*, vol. 45, no. 11, pp. 820–837, Nov. 2022, doi: 10.1016/j.tins.2022.08.007.
[34] P. Bak, C. Tang, and K. Wiesenfeld, “Self-organized criticality: An explanation of the 1/ *f* noise,” *Phys. Rev. Lett.*, vol. 59, no. 4, pp. 381–384, Jul. 1987, doi: 10.1103/PhysRevLett.59.381.
[35] L. Cocchi, L. L. Gollo, A. Zalesky, and M. Breakspear, “Criticality in the brain: A synthesis of neurobiology, models and cognition,” *Progress in Neurobiology*, vol. 158, pp. 132–152, Nov. 2017, doi: 10.1016/j.pneurobio.2017.07.002.
[36] M. A. Kramer, “Golden rhythms as a theoretical framework for cross-frequency organization,” *Neurons, Behavior, Data analysis, and Theory*, vol. 1, Oct. 2022, doi: 10.51628/001c.38960.
[37] E. Milotti, “1/f noise: a pedagogical review.” arXiv, Apr. 12, 2002. Accessed: Oct. 25, 2022. [Online]. Available: http://arxiv.org/abs/physics/0204033
[38] B. Caroli, C. Caroli, and B. Roulet, “High-frequency power spectra of systems described by non-linear Langevin equations,” *Physica A: Statistical Mechanics and its Applications*, vol. 112, no. 3, pp. 517–522, Jun. 1982, doi: 10.1016/0378-4371(82)90193-5.
[39] M. A. Colombo *et al.*, “The spectral exponent of the resting EEG indexes the presence of consciousness during unresponsiveness induced by propofol, xenon, and ketamine,” *NeuroImage*, vol. 189, pp. 631–644, Apr. 2019, doi: 10.1016/j.neuroimage.2019.01.024.
[40] F. S. Racz *et al.*, “Separating scale-free and oscillatory components of neural activity in schizophrenia,” *Brain and Behavior*, vol. 11, no. 5, p. e02047, 2021, doi: 10.1002/brb3.2047.
[41] A. Ibarra Chaoul and M. Siegel, “Cortical correlation structure of aperiodic neuronal population activity,” *NeuroImage*, vol. 245, p. 118672, Dec. 2021, doi: 10.1016/j.neuroimage.2021.118672.
[42] R. Chaudhuri, B. J. He, and X.-J. Wang, “Random Recurrent Networks Near Criticality Capture the Broadband Power Distribution of Human ECoG Dynamics,” *Cerebral Cortex*, vol. 28, no. 10, pp. 3610–3622, Oct. 2018, doi: 10.1093/cercor/bhx233.
[43] J. M. Beggs and D. Plenz, “Neuronal Avalanches in Neocortical Circuits,” *J. Neurosci.*, vol. 23, no. 35, pp. 11167–11177, Dec. 2003, doi: 10.1523/JNEUROSCI.23-35-11167.2003.
[44] K. Linkenkaer-Hansen, V. V. Nikouline, J. M. Palva, and R. J. Ilmoniemi, “Long-Range Temporal Correlations and Scaling Behavior in Human Brain Oscillations,” *J. Neurosci.*, vol. 21, no. 4, pp. 1370–1377, Feb. 2001, doi: 10.1523/JNEUROSCI.21-04-01370.2001.
[45] N. Adelhöfer *et al.*, “Increased scale-free and aperiodic neural activity during sensorimotor integration—a novel facet in Tourette syndrome,” *Brain Communications*, vol. 3, no. 4, p. fcab250, Oct. 2021, doi: 10.1093/braincomms/fcab250.

[46] P. Fransson, M. Metsäranta, M. Blennow, U. Åden, H. Lagercrantz, and S. Vanhatalo, “Early Development of Spatial Patterns of Power-Law Frequency Scaling in fMRI Resting-State and EEG Data in the Newborn Brain,” *Cerebral Cortex*, vol. 23, no. 3, pp. 638–646, Mar. 2013, doi: 10.1093/cercor/bhs047.
[47] W. J. Freeman, L. J. Rogers, M. D. Holmes, and D. L. Silbergeld, “Spatial spectral analysis of human electrocorticograms including the alpha and gamma bands,” *Journal of Neuroscience Methods*, vol. 95, no. 2, pp. 111–121, Feb. 2000, doi: 10.1016/S0165-0270(99)00160-0.
[48] G. Spyropoulos *et al.*, “Spontaneous variability in gamma dynamics described by a damped harmonic oscillator driven by noise,” *Nat Commun*, vol. 13, no. 1, Art. no. 1, Apr. 2022, doi: 10.1038/s41467-022-29674-x.
[49] W. J. Freeman, “Linear approximation of prepyriform evoked potential in cats,” *Experimental Neurology*, vol. 5, no. 6, pp. 477–499, Jun. 1962, doi: 10.1016/0014-4886(62)90058-4.
[50] H. R. Wilson and J. D. Cowan, “Excitatory and Inhibitory Interactions in Localized Populations of Model Neurons,” *Biophysical Journal*, vol. 12, no. 1, pp. 1–24, Jan. 1972, doi: 10.1016/S0006-3495(72)86068-5.
[51] A. Ghosh, Y. Rho, A. R. McIntosh, R. Kötter, and V. K. Jirsa, “Noise during rest enables the exploration of the brain’s dynamic repertoire,” *PLoS Comput Biol*, vol. 4, no. 10, p. e1000196, Oct. 2008, doi: 10.1371/journal.pcbi.1000196.
[52] R. F. Helfrich, A. Breska, and R. T. Knight, “Neural entrainment and network resonance in support of top-down guided attention,” *Current Opinion in Psychology*, vol. 29, pp. 82–89, Oct. 2019, doi: 10.1016/j.copsyc.2018.12.016.
[53] J. Taylor, *Classical Mechanics*. University Science Books, 2005.